JOURNAL OF GEOPHYSICAL RESEARCH, VOL. 104, NO. A11, PAGES 25,021-25,034, NOVEMBER 1, 1999

Generation of Pi2 pulsations by bursty bulk flows

Larry Kepko and Margaret Kivelson[1]
Department of Earth and Space Sciences, University of California, Los Angeles

Abstract. We present the first observations directly relating bursty bulk flows (BBFs) to Pi2 pulsations. At ISEE 2, a large earthward flow was observed. The Institute of Geological Sciences (IGS) magnetometer chain located at the same local time as ISEE 2 recorded Pi2 pulsations, slightly delayed relative to flow onset, consisting of a long-period (7-8 mHz) component associated with oscillations of the substorm current wedge. We demonstrate that the ionospheric current began to increase 90 s before the arrival of these Pi2 pulsations. We argue that this precursor was generated by earthward convection of plasma sheet plasma. Phase skips at midlatitudes on the nightside are associated with new flow bursts at ISEE 2. The Air Force Geophysics Laboratory (AFGL) magnetometer chain, which was located on the dusk flank, measured Pi2 pulsations that started ~90 s after the flow bursts. We demonstrate that there is a one-to-one correlation between impulsive flow onset in the tail and Pi2 pulsations. We also show that oscillations at AFGL are directly related to temporal variations of the flow. Thus we suggest that the characteristic frequencies of low-latitude Pi2 pulsations are established by the temporal structure of processes in the near-Earth magnetotail.

1. Introduction

It is generally accepted that Pi2 pulsations (periods of 40-150 s) observed on the ground occur precisely at substorm onset [*Saito*, 1969; *Saito et al.*, 1976; *Sakurai and Saito*, 1976; *Yoeman et al.*, 1994], but the exact mechanism producing the pulsations is still unknown. These pulsations are global, appearing at high-latitude stations in the auroral zone beneath the enhanced substorm electrojet, at midlatitude stations (L<~6) on the nightside, and over a broad range of local times at low-latitude (L<~4) stations. At low latitudes, Pi2 pulsations are frequently observed even on the dayside [*Sutcliffe and Yumoto*, 1989]. The high-latitude, auroral zone pulsations are generally largest in amplitude (tens of nanoteslas) and localized to areas of sudden brightenings of the aurora and intensifications of the westward electrojet [*Olson and Rostoker*, 1978; *Rostoker and Olson*, 1978; *Pashin et al.*, 1984]. The midlatitude pulsations, most commonly used for substorm onset identification, tend to be <10 nT in amplitude, and are observed within a few hours of local time near the meridian of the substorm current wedge [*Sakurai and McPherron*, 1983; *Singer et al.*, 1983]. They are associated with positive H bays. Current theories suggest that these pulsations originate from the disruption of the cross-tail current and are the Alfvén waves (carrying field-aligned currents) that establish the substorm current wedge [*Lysak and Dum*, 1983; *Baumjohann and Glassmeier*, 1984; *Southwood and Hughes*, 1985]. Pi2 pulsations at lower latitudes may originate from a field line oscillation at the plasmapause [*Saito et al.*, 1976] or from impulsive disturbances launched in the near Earth plasma sheet through tail current disruption [*Yumoto et al.*, 1989; *Pekrides et al.*, 1997]. How these disturbances generate Pi2 pulsations is still an open question.

[1]Also at Institute of Geophysics and Planetary Physics, University of California, Los Angeles

Paper number 1999JA900361.
0148-0227/99/1999JA900361$09.00

Most studies attempting to correlate Pi2 pulsations with in situ measurements have used data from the inner magnetosphere [e.g., *Osaki et al.*, 1998; *Yumoto et al., 1989*; *Takahashi et al.*, 1992, 1995; *Saka et al.*, 1996]. Processes in the midtail plasma sheet that may be responsible for generating the pulsations have not been directly linked to low-latitude Pi2 pulsations. We will provide evidence that relates low-latitude Pi2s to bursty bulk flows (BBFs). BBFs are short-lived, high-speed, convective plasma flows that have been observed in the inner plasma sheet [*Angelopoulos et al.*, 1992, and references therein]. These episodic bursts of high-speed flows, thought to be caused by transient, and perhaps localized, reconnection [e.g., *Sergeev et al.*, 1992], are responsible for most magnetotail flux and particle transport [*Angelopoulos et al.*, 1994].

High-speed flow bursts of several hundreds of kilometers per second are frequently observed near ISEE apogee (~23 R_E) but are rarely observed inside of 10 R_E [*Baumjohann et al.*, 1990; *Angelopoulos et al.*, 1994; *Shiokawa et al.*, 1997]. It is reasonable to expect the flows to be braked by rapidly rising magnetic pressure near the transition from tail to dipolar field lines [*Haerendel*, 1992; *Shiokawa et al.*, 1997]. The impulse created by the deceleration of the high-speed flow serves as a broadband source of compressional energy for the inner magnetosphere and has been postulated as the source that drives low-latitude Pi2 pulsations [e.g., *Yumoto et al.*, 1989]. It has been suggested that the compressional energy of the impulse couples to a plasmaspheric cavity mode [*Zhu and Kivelson*, 1989; *Allan et al.*, 1986, 1996; *Sutcliffe and Yumoto*, 1991].

In this paper we focus on an event on April 19, 1979. We present data for an interval that includes a BBF observed by ISEE 2 near X=-17 R_E. There were three distinct Pi2 events, separated by several minutes, and each concurrent with plasma sheet flow. For the first event, Pi2 pulsations appeared on the ground at midlatitude magnetometer stations, and an impulse was observed at low latitudes on the flank. midlatitude stations on the nightside also observed a precursor to the pulsations. The second event was observed as an impulse at low-latitude stations, and a phase skip was observed in midlatitude magnetograms. For the third event, compressional pulsations in

Table 1. Geographic and Geomagnetic Coordinates for the IGS Magnetometer Chain Stations Used in This Paper

Station Name	Abbreviation	Geographic		Geomagnetic		L	LT
		Latitude, °N	Longitude, °W	Latitude, °N	Longitude, °W		at 0000 UT
Tromso	Tr	69.66	18.95	66.91	117.58	7.2	0115
Oulu	Ol	65.11	25.49	61.72	117.96	4.5	0141
Nurmijarvi	Nu	60.51	24.66	57.63	113.73	3.4	0138
Hartland	Ha	51.00	-4.48	54.28	80.46	2.3	2342
Eskdalemuir	Es	55.32	-3.20	58.11	84.29	2.8	2347
Durness	Du	58.58	-4.76	61.46	85.03	3.5	2340
Lerwick	Le	60.13	-1.18	62.19	89.86	3.7	2355
Faroes	Fa	62.03	-6.78	65.03	86.02	4.5	2332

the Pi2 band were observed by GOES 2 and 3 and oscillations were observed by flank ground stations. Both were well correlated with temporal variations of the flow velocity measured by ISEE 2. We examine the timing and correlation of the observed signals and link the observations into a single phenomenological model.

2. April 19, 1979 Observations

The event that we will study in detail occurred on April 19, 1979, between ~2330-2350 UT. ISEE 2 was located in the midtail plasma sheet at (-17.0, -0.8, 0.5) R_E in aberrated GSM coordinates. GOES 2 and GOES 3 were at 1650 and 1400 LT, respectively. The positions of the Institute of Geological Sciences (IGS) and Air Force Geophysics Laboratory (AFGL) chains in both corrected geomagnetic (CGM) and geographic coordinates are listed in Tables 1 and 2, respectively. Figure 1a shows an equatorial mapping of the positions of the spacecraft and the ground stations. Both ISEE 2 and the IGS magnetometer chain were located near local midnight, while the AFGL chain and the GOES 2 (100.6 W longitude) and GOES 3 (135.2 W longitude) geosynchronous spacecraft were on the dusk flank. The positions of the ground stations and the GOES spacecraft have been mapped along field lines to the Z=0 GSM plane using the *Tsyganenko* [1989] model (with Kp=2). We have plotted in Figure 1b the nominal position of the auroral oval [*Holzworth and Meng*, 1975], the locations of the AFGL and IGS ground stations, and the spacecraft footprints mapped to the ground also using the *Tsyganenko* [1989] model.

2.1 Plasma Sheet Observations (ISEE 2)

Figure 2 shows field and plasma data from ISEE 2. Magnetic field data are in GSM coordinates at 0.25-s resolution. The plasma data at 12-s resolution are from the Los Alamos National Laboratory (LANL) two-dimensional (2-D) Fast Plasma Experiment (FPE). The velocity measurements are in spacecraft coordinates, which differ little from GSE. The bursty bulk flow (BBF), as defined by the *Angelopoulos et al.* [1992] criteria, is shaded in gray and lasts from 2334 to 2346 UT during a small drop in AL (Figure 3). The magnetosphere had been very quiet for 2 hours before this event, and AL drops to only -45 nT. The flow at ISEE 2 was positive (earthward) for the entire event, except for a small tailward flow at 2347 UT near the end of the BBF. In addition, the earthward component of the flow velocity during the first few minutes of the BBF (2335-2338) was oscillatory, with a period of ~50 s.

During the interval plotted in Figure 2, several flow bursts are evident. The first, labeled (A), peaked at 2328:40 UT (marked with a vertical solid line), roughly 6 min before the start of the nominal BBF. Because the flow was seen near the plasma sheet boundary layer (PSBL), with $B_x \approx B_{\mathrm{total}}$, one must consider whether this flow was PSBL flow, i.e., nearly field-aligned streaming particles accelerated at a distant neutral line. The flow was associated with a 5 nT increase in B_z, indicating partial dipolarization, and this dipolarization continued sporadically until the end of the BBF. B_y increased before the flow burst, consistent with the diversion of magnetic flux in front of a moving flux tube or bubble [*Chen and Wolf*, 1993; *Sergeev et al.*, 1996]. The flow burst is accompanied by a large increase in the number density to a level approximating that observed around 2342-2346 UT when ISEE 2 was in the central plasma sheet (CPS). The total pressure also increases. We therefore believe that flow burst (A) occurred when an inner plasma sheet flux tube undergoing dipolarization brought dense plasma to ISEE 2 at the outer edge of the plasma sheet. In the next section we will show that this flow burst was associated with an impulse observed by the AFGL chain at low L shell on the dusk flank, consistent with the interpretation of the flow as a transient, bulk plasma motion rather than streaming of plasma along the PSBL.

After the initial flow burst, a brief period of slower flow (100 km/sec) was followed successively by two very brief flow bursts

Table 2. Geographic and Geomagnetic Coordinates for the AFGL Magnetometer Chain

Station Name	Abbreviation	Geographic		Geomagnetic		L	LT
		Latitude, °N	Longitude, °E	Latitude, °N	Longitude, °E		at 0000 UT
Newport	New	48.3	117.1	55.2	299.6	3.1	1611
Rapid City	Rpc	44.2	103.1	54.1	317.3	2.9	1707
Camp Douglas	Cds	44.0	90.3	56.3	334.2	3.2	1758
Mount Clemens	Mcl	42.6	82.9	55.8	344.8	3.1	1828
Sudbury	Sub	42.2	71.3	55.8	1.9	3.0	1914
Lompoc	Loc	34.7	120.6	40.2	300.6	1.7	1557
Tampa	Tpa	27.8	82.5	40.7	344.9	1.7	1830

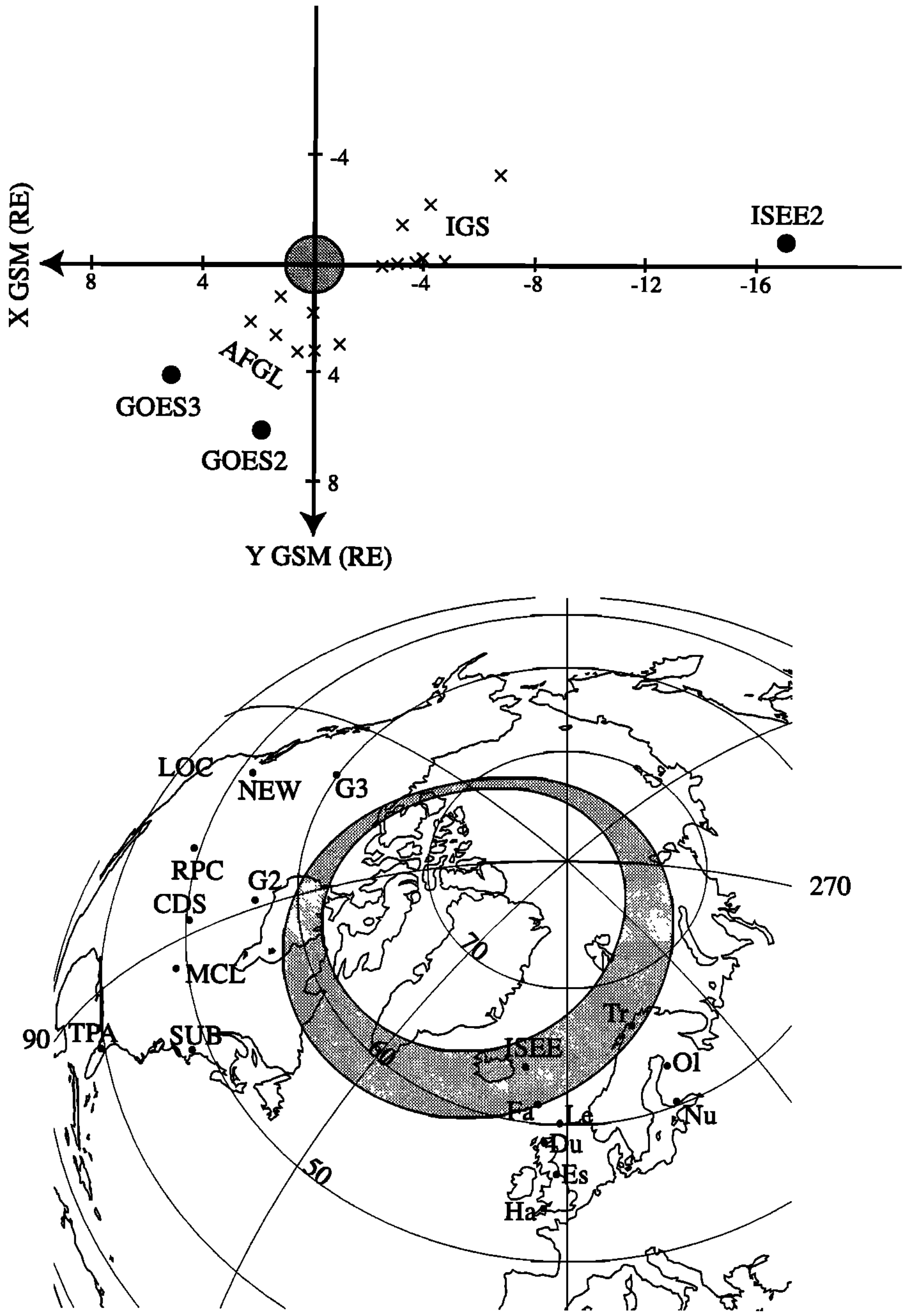

Figure 1. (a) Equatorial overview for the event of April 19, 1979. (b) Ground stations and satellite footprints for the event.

(labeled B and C) and by the BBF itself (flow D). Flow bursts B and C were observed closer to the center of the plasma sheet than flow burst A, as indicated by the decreasing value of $|B_x/B_z|$, and were not accompanied by changes in the number density. These bursts have some characteristics of streaming PSBL. As we will show, flow bursts B and D are associated with Pi2 oscillations observed at AFGL and GOES (burst D only), and with phase skips observed at IGS, whereas we find no activity to link to flow burst C. Thus we shall associate flow bursts A, B, and D with earthward flux transport in the central plasma sheet. Flow burst C contained a large V_y component, of the same order as V_x. We will return to this point later when discussing why burst C did not observe Pi2 pulsations.

2.2 Nightside Ground Observations (IGS)

We examined data from eight stations of the IGS magnetometer chain (Table 1), which was located near local midnight. The chain covers L shells from 2.3 to 7.2. Figure 4 shows the raw 2.5-s magnetic field *H* component (magnetic north) and *D* component (magnetic east) data for all eight stations. The V_x component of the velocity measured by ISEE 2 is placed at the top for reference. We know that most of the IGS stations map to approximately the same local time as ISEE 2 (Figure 1b). The *H* component data are consistent with this relationship. The five stations near 0° longitude show a positive (northward) *H* perturbation. Because these stations, with the

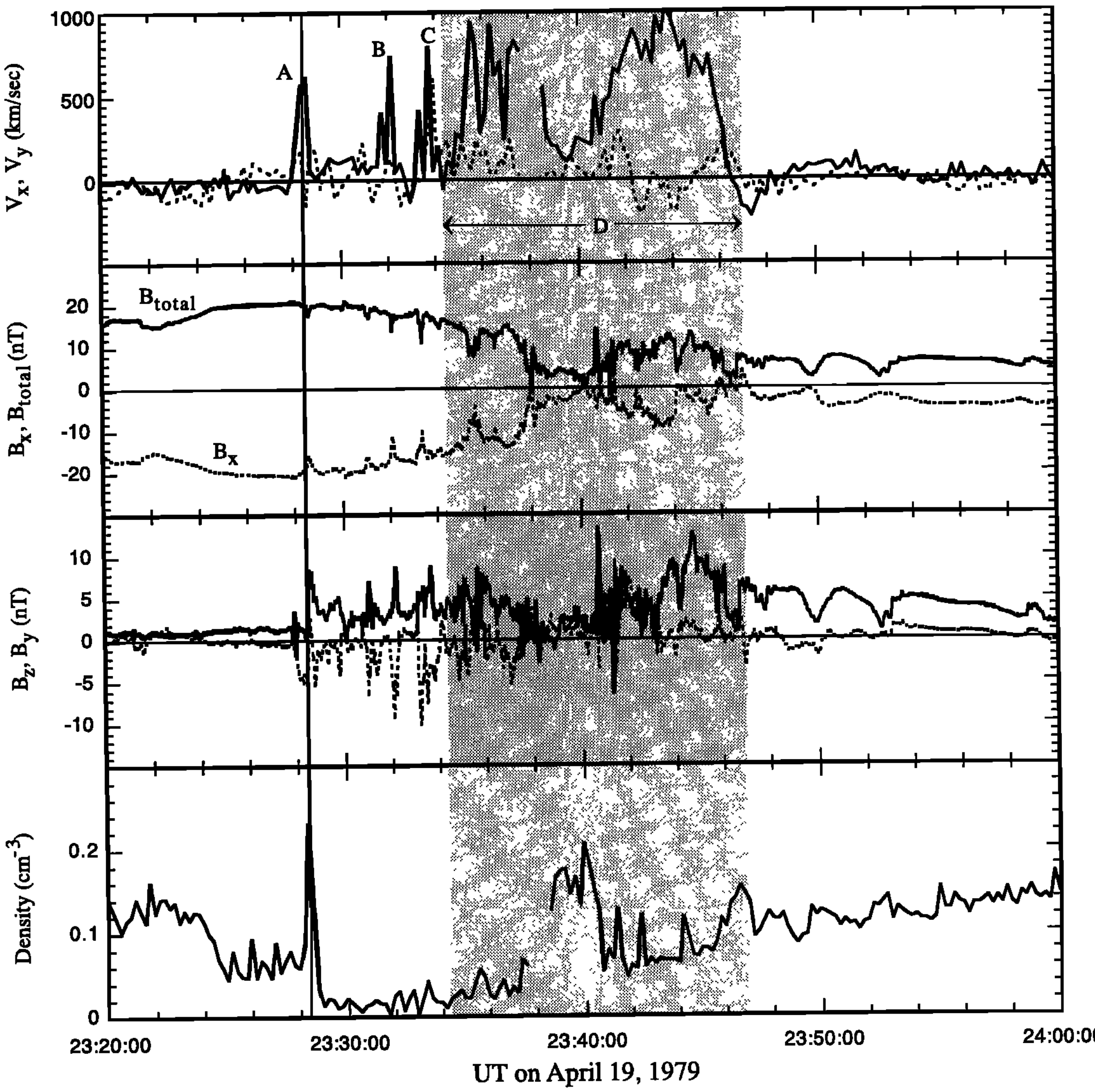

Figure 2. ISEE 2 measurements for April 19, 1979 bursty bulk flow (BBF). Plotted are the GSE velocity at 12-s resolution, 4-s GSM magnetic field, and the ion number density. V_x and B_z are plotted as solid lines, and V_y and B_y are plotted as dashed lines. The BBF as defined by *Angelopoulos et al.* [1994] is shaded grey (from 2334:22 to 2346:58 UT). The vertical line corresponds to the first peak in the velocity (2328:18 UT).

exception of Tromso, are at midlatitude, they do not observe perturbations due to currents flowing in the electrojet. Instead, they respond to a remote field-aligned current in space. The positive *H* perturbations places these five stations inside the substorm current wedge. Tromso (Tr), Olou (Ol), and Nurmijarvi (Nu) lie farther east and see a negative *H* perturbation implying that these stations lie outside the substorm current wedge.

There are two important points to note in the IGS data. First, the data start to deviate from a quiet background at 2328:18 UT simultaneous with the start of the first flow burst seen at ISEE 2 (the vertical line in Figure 2 and Figure 4). Second, there are phase jumps in the H-component (marked with downward arrows in Figure 4, and most evident in the middle traces). Comparison with the ISEE 2 flow data (Figure 4, top) shows that these phase jumps are roughly correlated with new flow bursts. We will examine the phase jumps in more detail later on.

2.3 Low-Latitude Flank Observations (AFGL)

The AFGL magnetometer chain consisted of seven stations, five near 55° corrected geomagnetic (CGM) latitude (*L*=3) across the northern United States, providing approximately three hours of local time coverage, and two near 40° CGM latitude (*L*=1.7) (see Table 2). Data are at 1-s resolution and are in *XY* coordinates, where *X* points to geographic north and *Y* to geographic east. The raw data are shown in Figure 5. Several events are evident. From 2324-2328 UT oscillations in the Pc3-4 band are observed, with the amplitude decreasing away from noon suggesting that the source was located on the dayside. A clear impulse in the direction of positive *X* is observed just after 2330 UT, followed by another at 2334 UT in the opposite direction. Oscillations with a period of ~45 s start at 2336 UT. The initial perturbation of these oscillations is in the negative *X* direction.

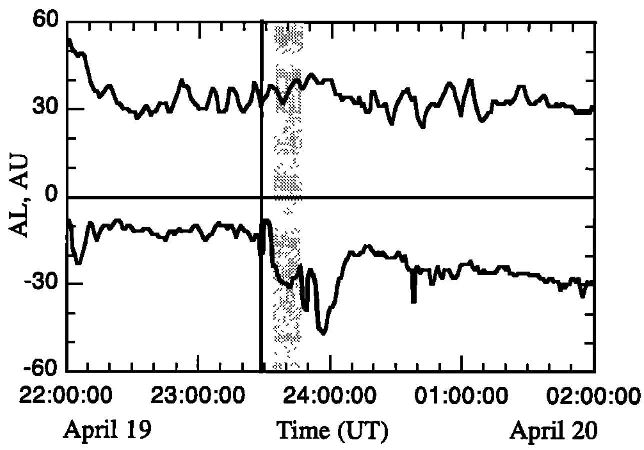

Figure 3. *AU* and *AL* indices for the April 19 BBF. The BBF (shaded in grey) and the first flow burst (solid line) occur just at the start of a slight *AL* decrease.

2.4 Magnetospheric Flank Observations (GOES)

The GOES 2 and GOES 3 geosynchronous satellites were located near the dusk flank at 100.6 W longitude (1700 LT) and 135.2 W longitude (1400 LT), respectively (Figure 1a). The magnetic field data are at 3-s resolution and are in a *VDH* dipole coordinate system, where *V* is outward and perpendicular to the dipole axis, *D* is eastward, and *H* is dipole field-aligned. Figure 6 presents the data from GOES 2, and also the power in the Pi2 band from three of the AFGL stations, and V_x measured at ISEE 2. Oscillations in the east-west (*D*) component with a period of ~50 s begin to increase in amplitude at 2336 UT (solid line), at the same time that AFGL observed the largest increase in power. There is also a slight increase in the outward (*V*) component. The total field exhibits a few oscillations between 2336 and 2339 UT. The data from GOES 3 (Figure 7) are extremely noisy, most likely from dayside wave activity, and show oscillations purely in the field-aligned component during the same interval that GOES 2 observed oscillations. The ratio of B_V to B_H indicates that GOES 3 was located near the magnetic equator while GOES 2 was several degrees above. Together, the GOES 2 and GOES 3 observations indicate that the compressional wave was confined to within a few degrees of the magnetic equator. In addition, the period of the field line resonances (50 s) observed at GOES 2 for tens of minutes after the Pi2 pulsations places the spacecraft outside the plasmasphere [*Cummings et al.*, 1969]. The time of the first increase at AFGL at 2330 UT is shown in both Figures 6 and 7 with a dashed line. Note that at this time there was no noticeable increase in the oscillation amplitude at either GOES spacecraft.

3. Discussion

3.1 Timing

The raw data from IGS, which was located near local midnight for this event, show linear changes in the *H* component starting at 2328:13 UT (Figure 8). This linear increase continues for ~90 s to 2329:43 UT, after which the perturbation field rises dramatically. All stations at IGS observe both the linear increase and the more rapid subsequent increase in the *H* component simultaneously, independent of local time or latitude. We will refer to these as Pi2 onsets 1 and 2 respectively. The ISEE 2 flow data (Figure 4, top) show that the flow began to increase 24 s (two samples) before the first Pi2 onset. The AFGL stations did not observe the precursor (onset 1), nor did they record clear oscillations like those observed at IGS. Instead, they detected an impulse near 2330 UT, ~20 s after onset 2 at IGS, and 2 min after onset 1 and flow burst A at ISEE 2. We will defer interpretation of these signals until the next section.

We have plotted in Figure 9 the components of the flow velocity measured at ISEE 2, the compressional component of the magnetic field from both GOES 2 and 3, and the *X* and *Y* components from the Mount Clemens (Mcl) station of the AFGL magnetometer chain for the interval during which Pi2 pulsations were observed (2335-2339 UT). The oscillations of the flow velocity at the beginning of the BBF (burst D) beginning at 2335 UT match the compressional oscillations measured at GOES 2 and GOES 3 and the ground oscillations observed at Mcl. The start of the oscillations occurs at ISEE 2 at 2335:08 UT and is observed ~40 s later at GOES 3. GOES 2 observes the impulse ~20 s after GOES 3, and the signal reaches the ground ~10 s later.

3.2 Nightside Phase Skips

Pi2 pulsations at high-latitude and midlatitude ground stations on the nightside often exhibit phase skips [e.g., *Meir-Jedrzejowicz and Hughes*, 1980]. Because phase skips are a change in phase of oscillations, they modify the cross-correlation coefficient, which is a measure of the phase coherence of the wave. In Figure 4, downward pointing arrows show where the cross correlation between the *H* and *D* components (not shown) drops to a minimum. The raw *H* component data confirm that these minima in polarized power correspond to phase skips. The second, at 2335:43 UT, is most noticeable, especially in the lowest latitude stations Ha, Es, and Du. The other phase skip is less evident but can be identified. The phase skips appear to be relatively closely associated with flow bursts B and D. The imperfect correlation may have several causes. The velocities in the flow bursts differ (for example, flow burst D was 200 km/sec faster than burst A). Also, the ISEE 2 footprint does not map exactly to the IGS chain (Figure 1b) and uncertainty in timing the start of a flow burst may contribute. In view of multiple timing uncertainties exact correlation is not anticipated, but the temporal relationship between flow bursts and phase skips suggests a causal link, a model that we investigate in the next section.

4. Interpretations

In this section we develop a qualitative model of the generation of Pi2 pulsations by fast earthward flow bursts in the magnetotail. The three Pi2 events analyzed in this paper, the first near 2330 UT, the second near 2334 UT and the third near 2336 UT, exhibit different characteristics that must be accounted for in any model. These characteristics include the following. First Pi2 at 2330 UT (flow burst A): (1) A single, impulsive flow burst at ISEE 2; (2) A precursor to the nightside, midlatitude Pi2 pulsations observed at IGS (near midnight, 57° to 67° geomagnetic latitude) lasting ~90 s and slightly delayed relative to the first measurement of flow in the midtail; (3) Oscillations in the range of 5-9 mHz observed at IGS, associated with a positive *H* bay; (Current theories link these oscillations to the

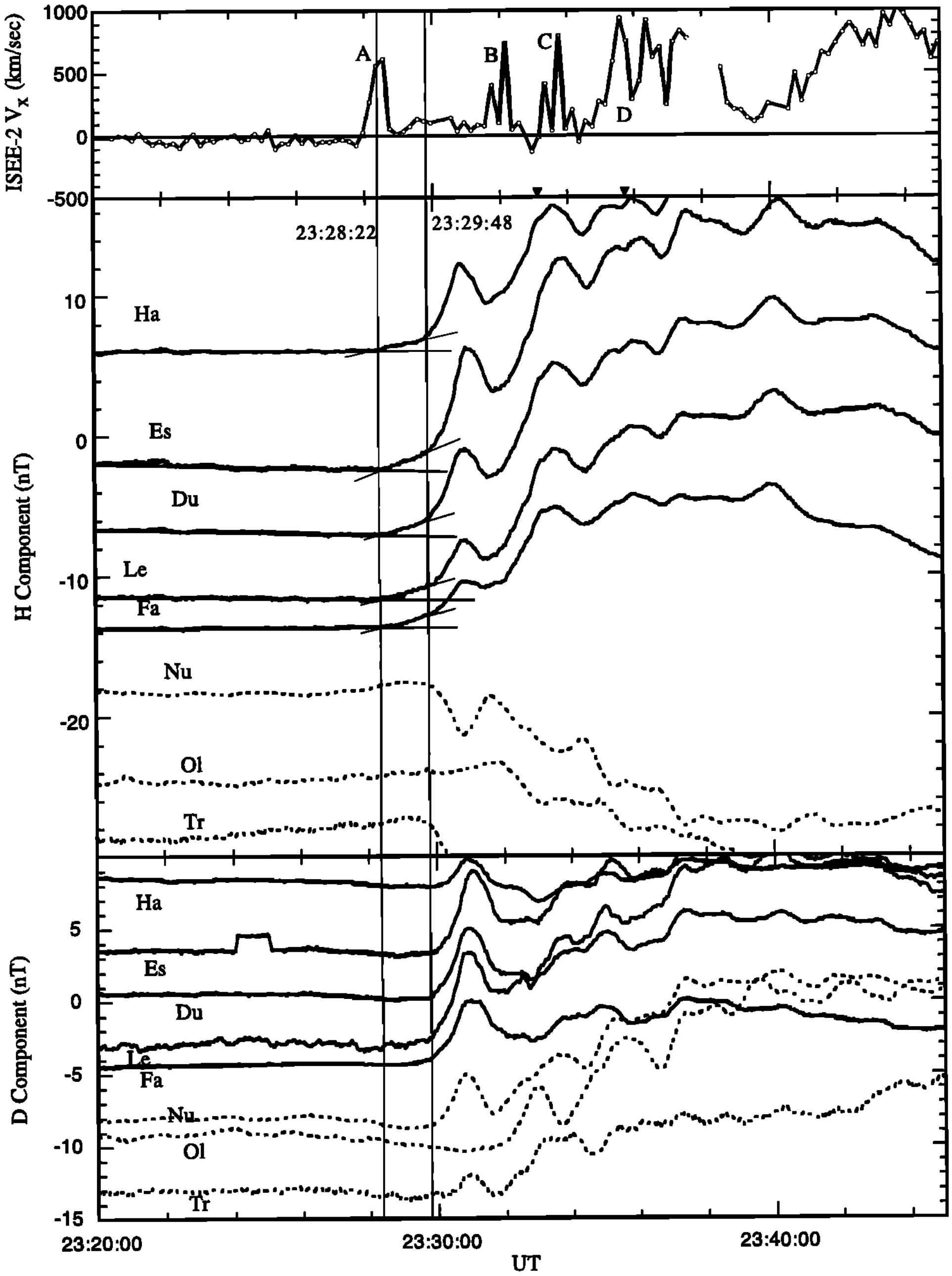

Figure 4. Raw 2.5-s *H* and *D* component magnetic field data from the IGS magnetometer chain on April 19, 1979. A baseline shift has been applied to all signatures. The first signature of field-aligned current is at 2328:22 UT (first vertical line), while the Pi2 began 90 s later (second vertical line). Downward arrows correspond to clear phase skips as identified by polarized power, and these have been shifted (upward arrows) by the delay time between ISEE 2 flows and Pi2 (90 s).

transient development of the substorm current wedge, and we adopt this interpretation.); (4) A single impulse in the positive *X* direction at AFGL (near dusk, 40° to 57° geomagnetic latitude), delayed slightly relative to the IGS pulsations; and (5) Neither detectable wave power nor an impulse at GOES 2 or 3. Second and Third Pi2 at 2334 and 2336 UT (flow bursts B and D): (1) Impulsive flow burst at ISEE 2 for flow B and oscillatory flow for burst D; (2) Phase skips at IGS for both bursts, but no obvious increase in the wave power or the field-aligned currents flowing overhead; (3) A single impulse in the negative *X* direction at near-dusk ground stations at AFGL for burst B. For burst D, oscillations near 15-20 mHz, with the frequency independent of latitude, and well correlated with temporal oscillations of the flow velocity measured at ISEE 2. The initial perturbation is also in the negative *X* direction; (4) Compressional oscillations observed by GOES 2 and GOES 3, for burst D only, also well correlated with temporal oscillations of the flow velocity measured at ISEE 2.

Our interpretation will require that the Pi2 pulsations be directly linked to the flows measured at ISEE 2. We must also account for the delays between the signals at four separate points: the midtail (ISEE 2), nightside midlatitude (IGS), ground

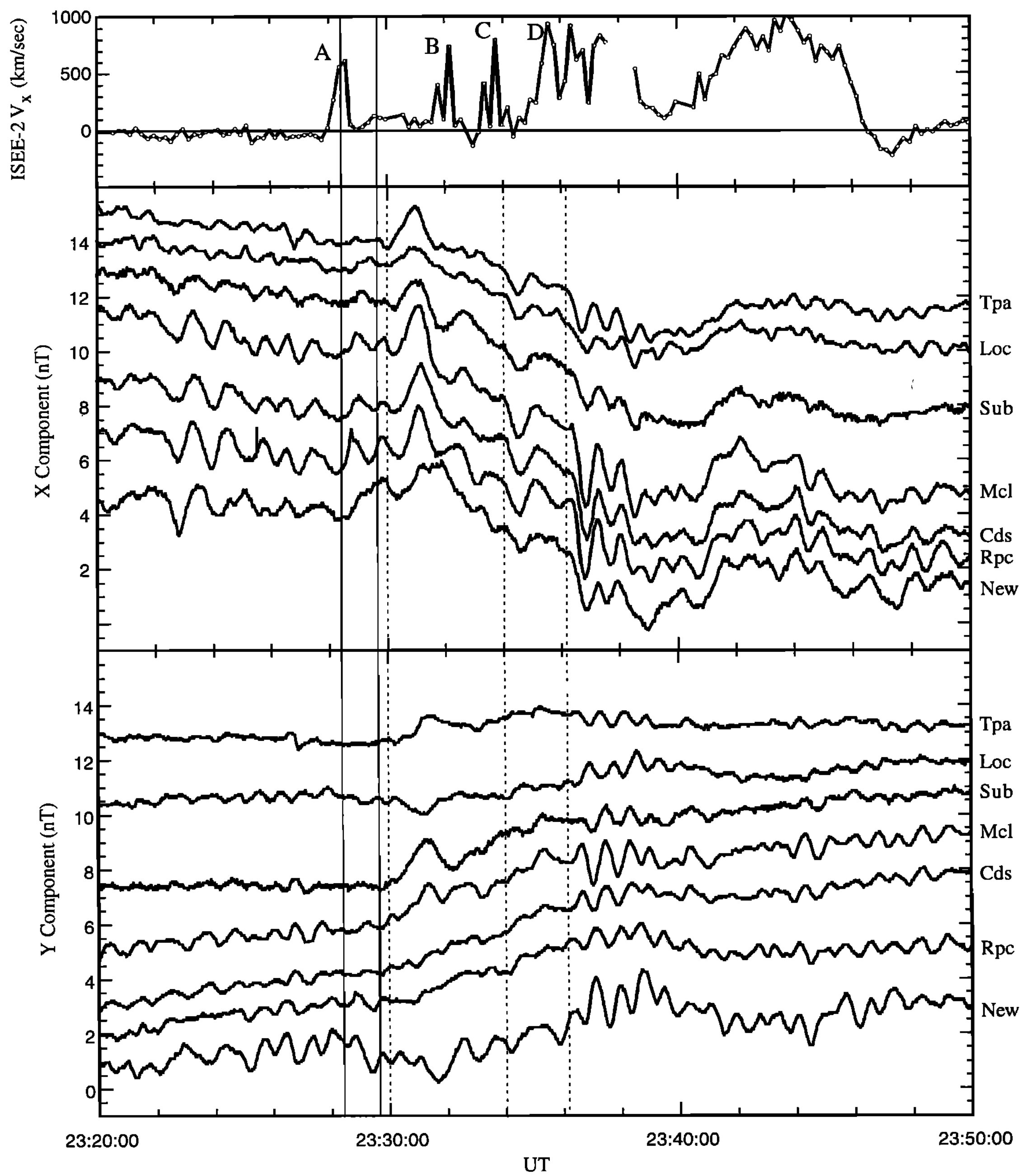

Figure 5. Raw AFGL data at 1-s resolution on April 19, 1979. Data are in *XY* (geographic) coordinates. A baseline shift has been applied to all signatures. The solid vertical lines are the same as in Figure 4. Dashed lines are the Pi2 onsets.

flank (AFGL), and magnetospheric flank (GOES) for all of which we have quantitative estimates. Finally, our interpretations must be consistent with results of previous Pi2 research. In the next few sections we incorporate all of these observations and constraints into a single phenomenological model.

4.1 midlatitude Pi2 Precursor

The IGS data show what we term a Pi2 precursor, beginning at 2328:22 UT (Figure 8). We believe this precursor indicates the changed ionospheric convection in the midlatitude, near midnight sector that develops when an event in the magnetotail, probably reconnection, initiates an earthward traveling flow burst. The electric field associated with the magnetospheric convection maps to the ionosphere where it provides the $\boldsymbol{J} \times \boldsymbol{B}$ force needed to move the ionospheric footprint equatorward. We estimate the magnitude of this current and show that it is consistent with the observed magnetic signatures. The convective electric field of the flow, $\boldsymbol{E}_C = -\boldsymbol{V} \times \boldsymbol{B}$, is applied to the ionosphere where it drives a Pedersen current

$$j_P = \Sigma_P E_I. \tag{1}$$

Here Σ_P is the height integrated Pedersen conductivity, E_I is the ionospheric electric field, related to the convective electric field in the tail by a geometric scaling factor, and j_P is the linear Pedersen current density in units of amps/m. The total perturbation current flowing in the ionosphere is

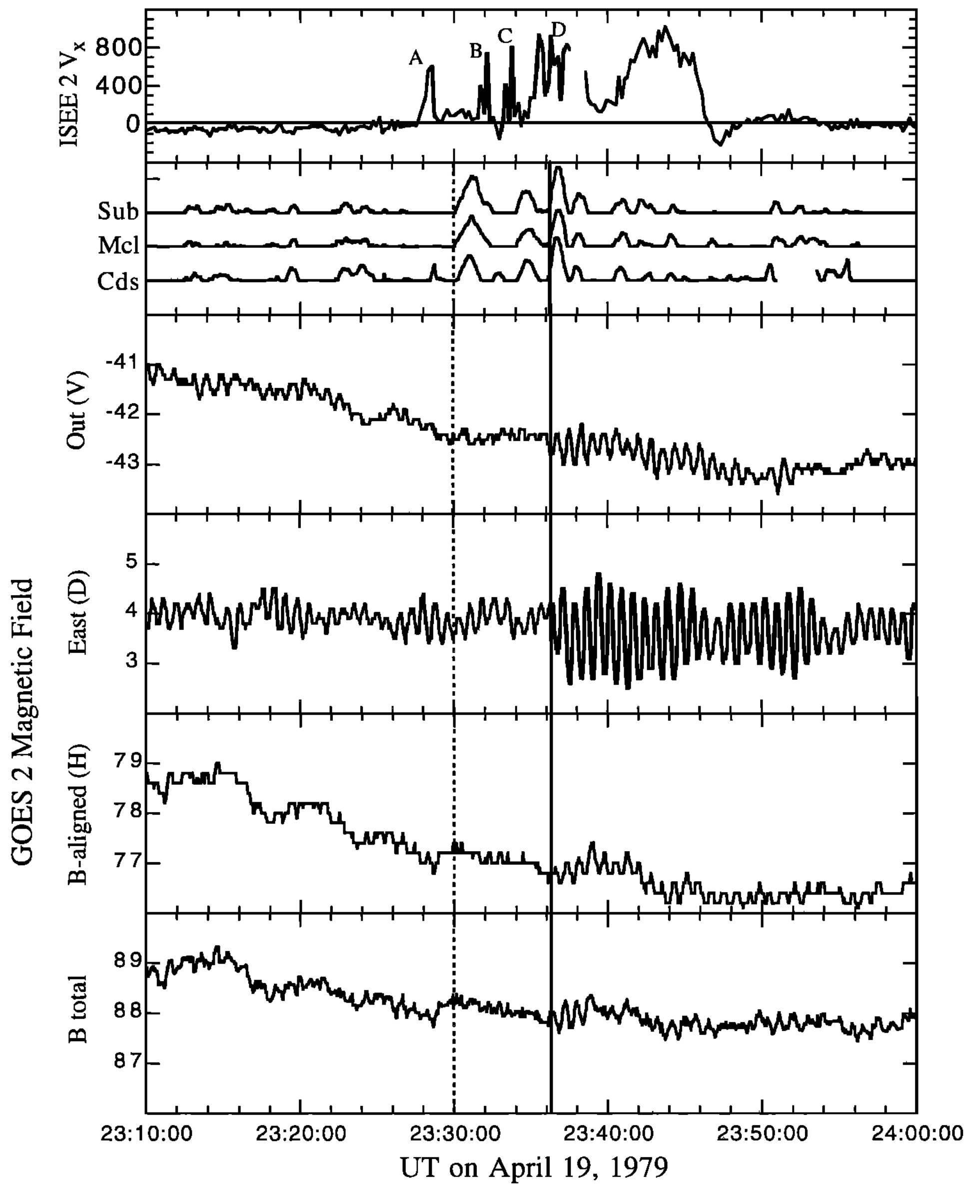

Figure 6. GOES 2 data (3-s resolution) in *VDH* coordinates for the April 19 event. The dashed line is the time of the first Pi2 observed at AFGL, and the solid line is the time of the second Pi2 at AFGL. Note the increase in wave activity after 2336.

$$I_P = \Sigma_P E_I dx, \quad (2)$$

where dx is the north-south width of the current, which is simply the projection of the radial length of the flow channel onto the ionosphere. The scaling factor that relates the ionospheric electric field to the convective electric field is dy_M/dy_I, where dy_M is the east-west width of the flow channel in the magnetosphere and dy_I is the width of dy_M projected onto the ionosphere. Equation (2) becomes

$$I_P = \Sigma_P V_{BBF} B_{tail} \frac{dy_M}{dy_I} dx. \quad (3)$$

Using upper limit estimates of Σ_P=10 mhos, V_{BBF}=1000 km/s, B_{tail}=10 nT, dy_M=2 R_E, dy_I=1500 km, and dx= 200 km, we obtain $I_P \sim 10^5$ amps, which is an order of magnitude lower than the typical substorm current wedge magnitude of 10^6 amps. Directly beneath this current the magnetic perturbation would be a few tens of nanoteslas. The IGS stations, as in the case of the substorm current wedge, would measure perturbations due to the field-aligned section of this current system. The perturbation at these stations is typically reduced by a factor of 10-20 compared to measurements directly beneath the current. Figure 4 shows that the Pi2 precursor is < 2 nT, consistent with our crude estimate.

4.2 Nightside midlatitude Pi2 Pulsations

As the flow in the plasma sheet reaches the region in which the magnetic configuration changes from a stretched tail to dipolar field lines, it is braked by the rapid increase in magnetic pressure at the dipolar/tail boundary [*Haerendel*, 1992; *Shiokawa et al.*, 1997]. This braking can generate up to 10^5 amps [*Shiokawa et al.*, 1998], in the same sense as the substorm current wedge. Additional field-aligned currents are generated

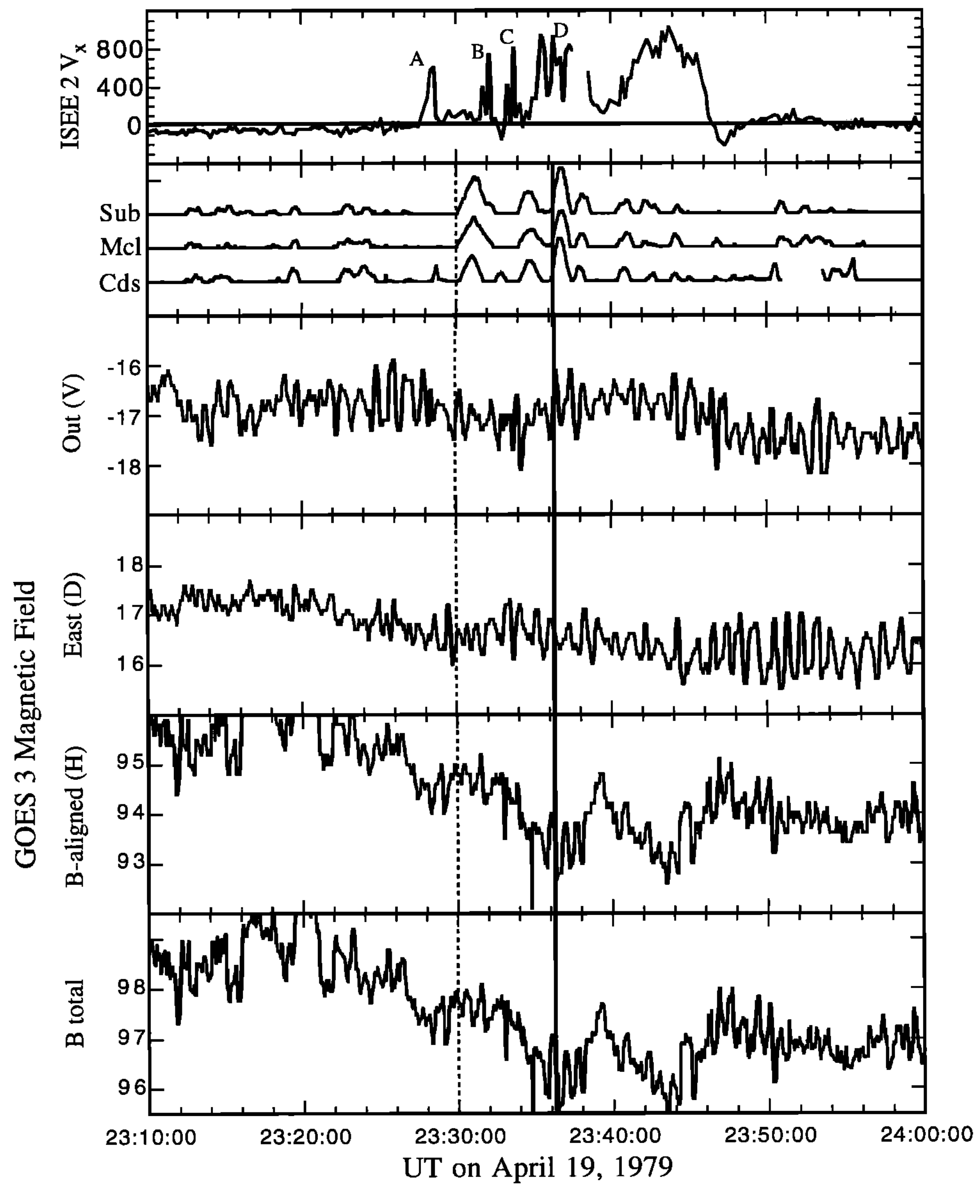

Figure 7. GOES 3 data (3-s resolution) in the same format as Figure 6.

by magnetic shear and azimuthal pressure gradients [*Birn and Hesse*, 1996]. While this current is referred to as the substorm current wedge, the event studied here was not a substorm, but the sense and general features of the current is the same. The Pi2 pulsations result from a partial reflection by the ionosphere of this field-aligned current and are the transient response of the magnetosphere-ionosphere system as it responds to changing flows [*Lysak and Dum*, 1983; *Baumjohann and Glassmeier*, 1984; *Southwood and Hughes*, 1985]. The 100-s period of the oscillations is determined by the time required for the wave to travel from the equator to the ionosphere and back to the equator. The waves die out once flows have been established in the ionosphere, typically within a few cycles.

This interpretation provides a simple explanation for the phase skips observed at nightside midlatitude stations. Each flow burst carries magnetic flux and plasma to the braking region where the substorm-like currents, including field aligned currents, begin to flow. Prior to the initial flow burst, ionospheric convection must have been absent or slow. The strong Pi2 pulsations observed by IGS (i.e., a strong reflection of field-aligned current) developed as the ionosphere was set into motion. Flow bursts B and D generated a new field-aligned current leading to the formation of a new pulsation packet, superimposed on existing Pi2 pulsations. Depending on the phase and amplitude of the existing pulsations and the amplitude of the new signal, we can observe a clear phase skip (such as at 2335:43 UT) or a subtle phase skip (such as at 2332:42 UT).

4.3 Inner magnetospheric Oscillations

The three pulsation events observed at low latitudes on the flank exhibit very different characteristics. The first at 2330 UT was observed as a single impulse in the positive *X* direction on the ground but was not observed by either GOES spacecraft. The second at 2334 UT was observed as a single impulse in the negative *X* direction, opposite that of the first Pi2. The third Pi2 at 2336 UT appeared as a series of three pulsations and was observed both on the ground and at GOES (as compressional

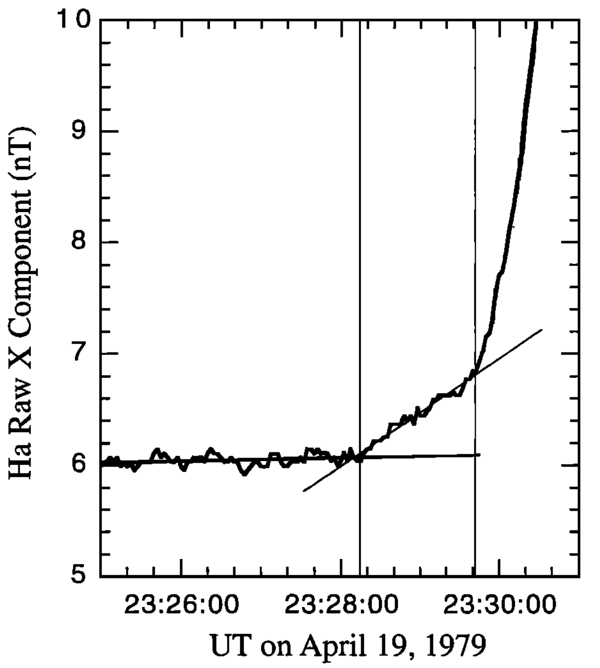

Figure 8. The Pi2 precursor observed by IGS. The linear increase starts near 2328 UT and continues for ~90 s before the start of the Pi2.

oscillations). The initial deflection at AFGL was also in the negative X direction. The quality of the correlation of the temporal variations of the flow velocity in the midtail to the Pi2 waveforms measured at low-latitude stations on the flank for the third Pi2 (Figure 10) suggests a direct link between the two. The timing of the signals (Figure 9) also is consistent with the proposal that the flows are the source of the pulsations. Yet existing theories on low-latitude Pi2 pulsations do not directly link the pulsations to temporal variations of magnetotail flow bursts but instead relate them to plasmaspheric cavity mode oscillations [e.g., *Lee*, 1998; *Sutcliffe and Yumoto*, 1989] or surface waves on the plasmapause [*Saito et al.*, 1979; *Chen and Hasegawa*, 1974].

Studies of low-latitude Pi2 pulsations using in situ spacecraft have not supported either the surface wave or cavity-mode models. Recently, *Osaki et al.* [1998] have examined Pi2 pulsations observed in the plasmasphere by the Akebono satellite. Based on Poynting flux measurements they found that a cavity mode could not sustain pulsations for more than a few seconds. *Takahashi et al.* [1992] studied plasmaspheric Pi2 pulsations using the AMPTE/CCE spacecraft. They found little evidence for compressional oscillations inside the plasmasphere outside of ± 3 hours of local midnight. Both studies suggested that a source localized near midnight would be required to explain low-latitude Pi2 pulsations, and that it would have to drive several cycles before damping out. *Osaki et al.* [1998] suggested that a source of energy external to the plasmasphere was required. On the basis of numerical modeling, *Itonaga et al.* [1997] argued that an external, oscillatory source incident on the plasmapause was required.

A possible source of compressional energy for the plasmasphere is directly provided by the braking of fast flows. Compression of the inner magnetosphere by a flow burst should generate a compressional wave traveling sunward [e.g., *Yumoto et al.*, 1989]. Figure 11a represents a simplified picture of the effect of an equatorally confined fast-mode wave ($k_\perp$) at the flank, where AFGL was located. The sunward-propagating disturbance perturbs the field lines azimuthally (locally along $\hat{x}$), with the perturbation field, δb, pointing antisunward in the northern hemisphere. We assume that this perturbation propagates Alfvénically along the field ($k_\parallel$), although both compressional and Alfvénic components will propagate parallel to the field. As the Alfvén wave reaches the ionosphere the perturbation rotates northward by 90° [*Hughes,* 1974], and this matches the observed perturbation on the ground. Thus a flow-driven impulsive compression provides a plausible explanation for the first impulsive Pi2 event associated with flow burst A.

Since neither GOES satellite observed a perturbation, we must conclude that the compressional impulse generated by the braking process in event A was confined to the plasmasphere. This is not an unreasonable assumption if the braking region is near the plasmapause.

While this picture explains event A, events B and D are quite different. The initial perturbation at AFGL is in the negative X direction, that is, southward rather than northward, for both events. Event D was observed by GOES 2 and 3, which were located outside the plasmasphere, in addition to AFGL. The model must explain two critical observations. It must account for the polarization of the initial deflection at AFGL for both events. It must also explain why GOES 3, located furthest sunward (see Figure 1), observed the pulsations associated with flow D before GOES 2.

The paradox of GOES 3 observing the oscillations before GOES 2 can be explained by the modification of wavefronts by nonuniform fast-mode velocity between the source region and the two spacecraft. This is shown in Figure 12. We adopt a fast-mode velocity profile with a plasmapause at 5 R_E, and assume azimuthal symmetry. Only the variations (not the absolute value) of the fast-mode velocity are important, as we are interested in the shape of the wave fronts and the spatial profile determines that shape. We note that the shape of the wave fronts at low-latitudes is very sensitive to the velocity profile adopted in that region. We started a sunward oriented perturbation at midnight at X=-7.5 R_E and followed it in all directions, recalculating the fast-mode velocity at each new position. The line-of-sight path to GOES 2 lies along the plasmapause, where the fast-mode velocity is minimum. This delays the arrival of the signal at GOES 2 and consequently GOES 3 observes the signal first. AFGL observes the signal further delayed by the time-of-flight from the equator to the ionosphere. At 3.5 R_E, this time is ~4 R_E/ 10^3 km/s ~ 30 s.

Consider now the initial perturbation of the Pi2 signal measured on the ground by AFGL at 2330 UT (event A). In the initial impulse, the perturbation field in the magnetosphere was directed antisunward. Rotation through the ionosphere then produced a northward perturbation on the ground directly beneath the wave. This accounts for the polarization of the first Pi2. However, the polarization of the ground signal becomes more complex for a radially localized magnetospheric compressional wave that links to a limited range of latitudes on the ground. In Figure 11b, we show the Pedersen and Hall currents generated by a latitudinally localized Alfvén wave. Directly below the Hall currents associated with the wave, a ground station would observe the usual 90° counterclockwise rotation (as observed from above). However, if the station were situated either north or south of the edge of the disturbance, it would observe a clockwise rotation (as observed from above). An antisunward perturbation would then be observed as a

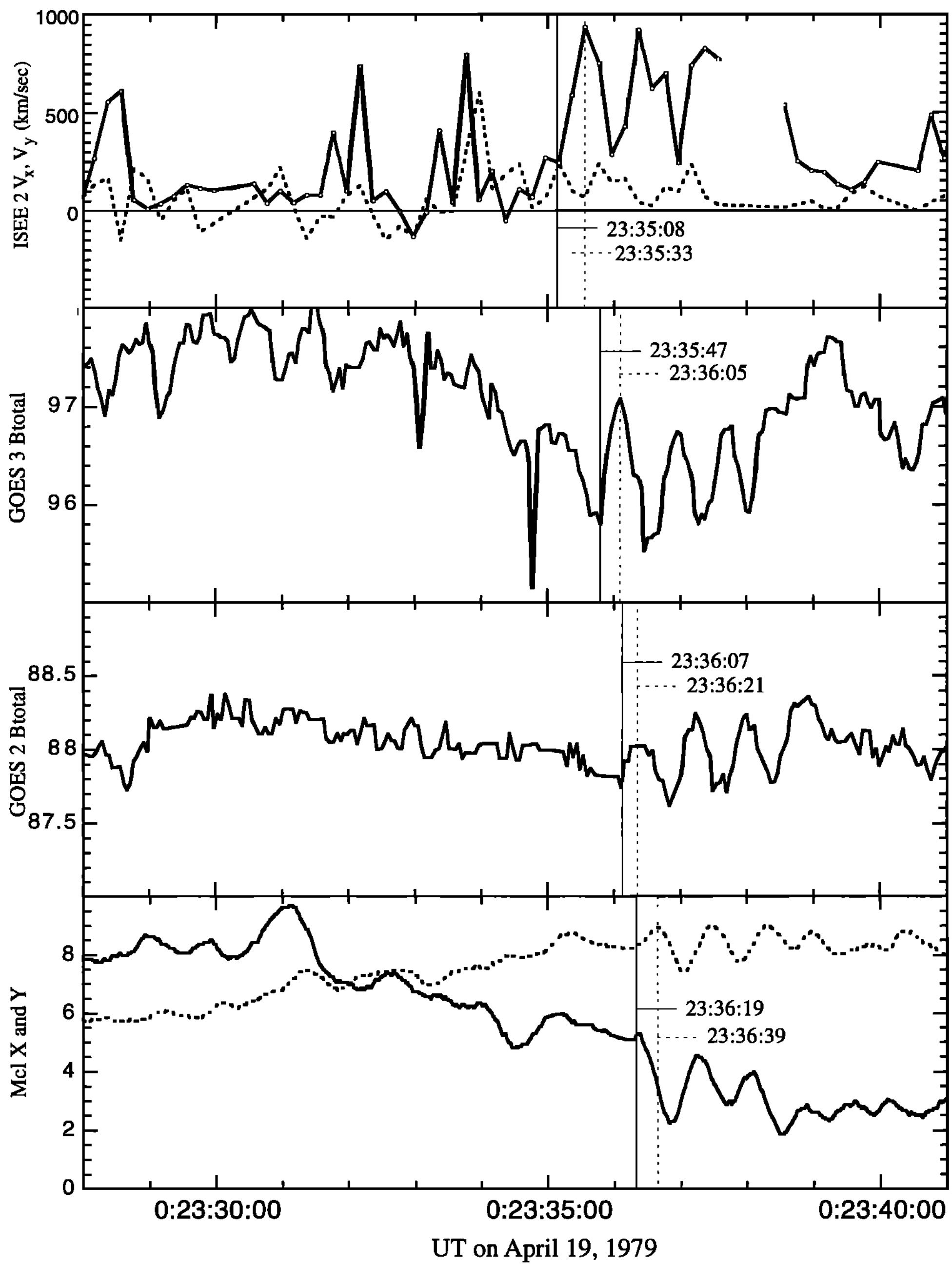

Figure 9. Timing of the third Pi2 signal observed in the ISEE 2 flow velocity, the GOES 2 and 3 total magnetic field, and AFGL (one station shown).

southward (negative X) perturbation on the ground, which was observed at AFGL for the second event. The GOES observations clearly indicate that compressional power was present outside the plasmasphere, on field lines located poleward of the AFGL chain. We unfortunately do not have in situ measurements on AFGL field lines that fall within the plasmasphere to determine if the compressional wave power was low there.

There is also the question of why GOES observed the third Pi2 event but not the first two One possibility is that the wave power was small compared to the background noise. A second possibility is that the braking region was modified by the first flow burst so that braking occurred differently, or in a different region. We note that *Angelopoulos et al.* [1996] found that a BBF creates an azimuthally localized region of dipolarization in the inner magnetosphere. A BBF arriving a few minutes later would then been deflected east and west before being braked, thus directing the compressional energy more toward the flanks. This could explain the difference in polarization between the first Pi2 at AFGL and the last two. This may also explain why the second BBF, while creating large signals at AFGL and GOES on the flanks, was not clearly observed on the nightside by IGS. Finally, our interpretation provides an explanation for why flow burst C, if not PSBL flow, was not associated with any Pi2 pulsations. Burst C contained a significant V_y component and never reached the braking region and therefore did not generate the compressional pulse necessary for low-latitude Pi2.

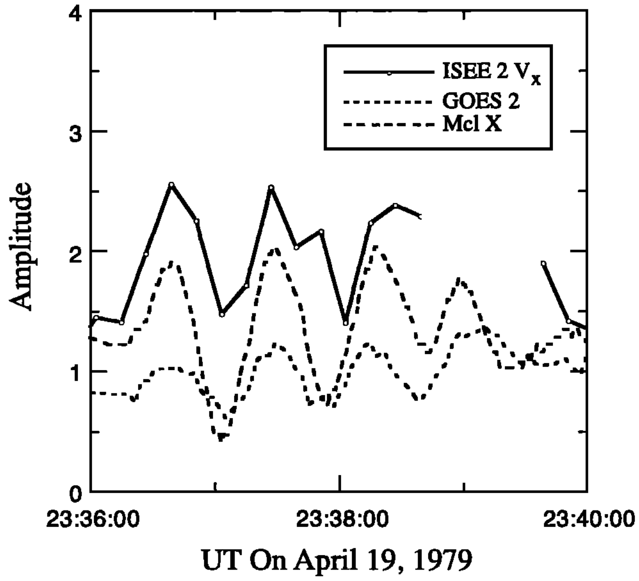

Figure 10. Data from the Pi2 starting at 2336 UT showing good correlation between the oscillations at widely separated points. The ISEE 2 flow velocity has been shifted 65 s and the GOES data have been shifted 15 s to account for propagation delays. No time shift was applied to the Mount Clemens (Mcl) data.

5. Summary

Pi2 pulsations are regarded as an accurate signature of the initiation of activity in the geomagnetic tail. However, the process that initiates the pulsations has not been unambiguously identified. We have used ground data from the AFGL and IGS magnetometer chains combined with in situ measurements by GOES 2 and 3 and timed Pi2 pulsations relative to the observation of flows at ISEE 2. We have focused on an event associated with a very low level of disturbance that occurred during low geomagnetic activity, to avoid any uncertainty that might arise due to multiple flow channels or from previous activity. We summarize our results:

1. There appears to be a nightside, midlatitude precursor to Pi2 pulsations due to inward convection from the distant magnetotail. This precursor is observed as a linear increase in the horizontal perturbation field, and persists for ~90 s.

2. If oscillations are already present, each new flow burst creates a phase skip in nightside midlatitude pulsations.

3. There is a one to one correlation between Pi2 pulsations at low latitudes on the flank and flow bursts in the magnetotail, delayed by ~2 min.

4. Low-latitude pulsations are driven by temporal variations of flows in the magnetotail.

Using our observations and building upon the work of previous research, we have linked the elements that account for mid-latitude and low-latitude Pi2 pulsations. We argue that there is a direct link between earthward convection produced by a BBF and the wave signals. The first indication of geomagnetic activity is the Pi2 precursor, which we believe is associated with the earthward convection of flux tubes from the distant magnetotail. Near midnight, enhanced earthward flows in the plasmasheet precede the impulses on the ground. Upon reaching the inner magnetosphere, the flow is braked and the combination of braking current, magnetic shear, and pressure gradients create a current system analogous to the substorm current wedge. Midlatitude Pi2 pulsations on the nightside arise as the transient response of the ionosphere to this current system. The braking generates a compressional wave that drives waves at low-latitude ground stations. If the flow velocity is periodic, then the compressional waves from the braking is as well. The periodicity is extrinsic to the inner and middle magnetosphere and is controlled by magnetospheric processes in the geomagnetic tail. On the flanks, the compressional waves drive Alfvén waves and thereby drive directly low-latitude Pi2s.

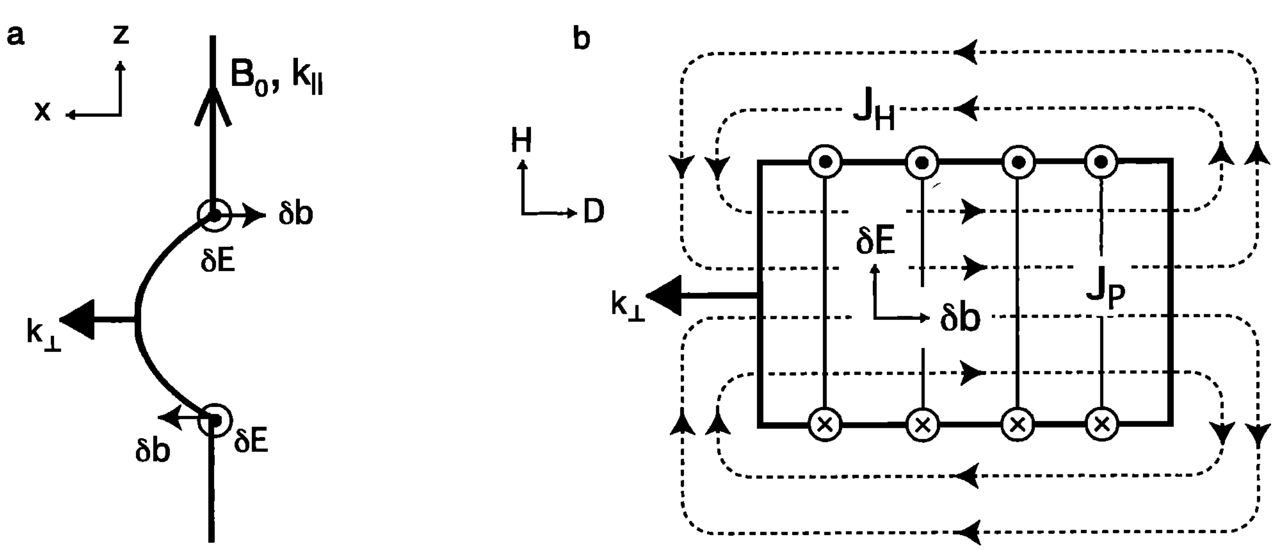

Figure 11. (a) The effect of an equatorally confined fast-mode wave ($k_\perp$) striking field lines azimuthally. The impulse creates a kink in the field line which is assumed to propagate as an Alfvén wave ($k_{\|}$) to the ionosphere. (b) The Hall currents (solid lines) and Pedersen currents (dashed lines) in the ionosphere created by an azimuthally limited Alfvén wave.

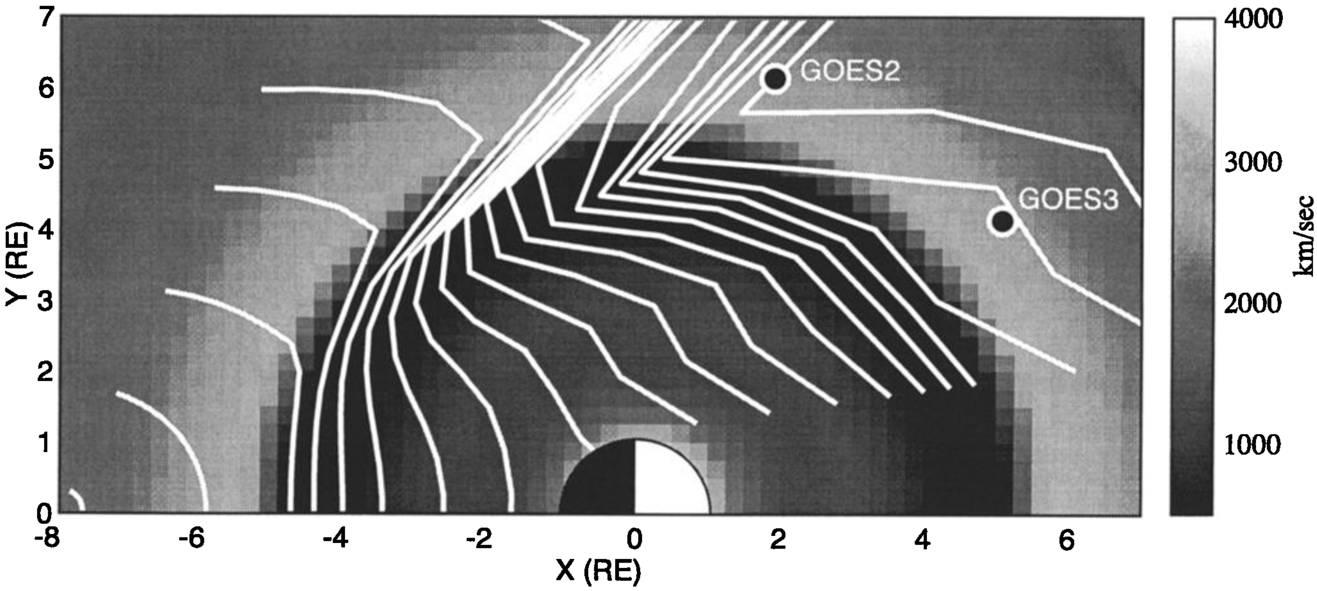

Figure 12. Explanation for the difference in timing between the GOES spacecraft. We assume an azimuthally symmetric fast-mode velocity profile, with a minimum near the plasmapause. A compressional signal was then started on the nightside and allowed to propagate sunward. Note that the signal arrives at GOES 3 before GOES 2.

Acknowledgments. The authors thank R. L. McPherron and K. K. Khurana for many helpful discussions. Additional interactions with colleagues at the Geospace Environment Modeling workshops have added greatly to this work. We would like to thank C. T. Russell for providing ISEE 2 magnetic field data and Los Alamos National Laboratory for ISEE 2 plasma data. GOES data were provided by the National Oceanographic and Atmospheric Administration. We are grateful to C. T. Russell for archiving the ground data and making them available for use. This work was supported by the National Science Foundation under grant ATM 93-14239 and the Los Alamos Division of the Institute of Geophysics and Planetary Physics, UCRP 708.

Janet G. Luhmann thanks Kazuo Shiokawa and Peter R. Sutcliffe for their assistance in evaluating this paper.

References

Allan, W., E. M. Poulter, and S. P. White, Hydromagnetic wave coupling in the magnetosphere — Plasmapause effects on impulse-excited resonances, *Planet. Space Sci.*, *34*, 1189-1200, 1986.

Allan, W., F. W. Menk, B. J. Fraser, Y. Li, and S. P. White, Are low-latitude Pi2 pulsations cavity/waveguide modes?, *Geophys. Res. Lett.*, *23*, 765-768, 1996.

Angelopoulos, V., C. F. Kennel, F. V. Coroniti, R. Pellat, M. G. Kivelson, R. J. Walker, W. Baumjohann, G. Paschmann, and H. Lühr, Bursty bulk flows in the inner central plasma sheet, *J. Geophys. Res.*, *97*, 4027, 1992.

Angelopoulos, V., C. F. Kennel, F. V. Coroniti, R. Pellat, M. G. Kivelson, R. J. Walker, C. T. Russell, W. Baumjohann, W. C. Feldman, and J. T. Gosling, Statistical characteristics of bursty bulk flow events, *J. Geophys. Res.*, *99*, 21257, 1994.

Angelopoulos, V., et al., Multipoint analysis of a bursty bulk flow event on April 11, 1985, *J. Geophys. Res.*, *101*, 4967-89, 1996.

Baumjohann, W., and K. H. Glassmeier, The transient response mechanism and Pi2 pulsations at substorm onset — Review and outlook, *Planet. Space Sci.*, *32*, 1361-1370, 1984.

Baumjohann, W., G. Paschmann, and H. Lühr, Characteristics of high-speed ion flows in the plasma sheet, *J. Geophys. Res.*, *95*, 3801-3809, 1990.

Birn, J., and M. Hesse, Details of current disruption and diversion in simulations of magnetotail dynamics, *J. Geophys. Res.*, *101*, 15345-58, 1996.

Chen, C. X., and R. A. Wolf, Interpretation of high-speed flows in the plasma sheet, *J. Geophys. Res.*, *98*, 21409, 1993.

Chen, L., and A. Hasegawa, A theory of long period magnetic pulsations, 2, Impulse excitation of surface eigenmode, *J. Geophys. Res.*, *79*, 1033-1037, 1974.

Cummings, W. D., R. J. O'Sullivan, and P. J. Coleman, Standing Alfvén waves in the magnetosphere, *J. Geophys. Res.*, *74*, 778-793, 1969.

Haerendel, G., Disruption, ballooning or auroral avalanche — On the cause of substorms, *Proc. of the International Conference on Substorms (ICS-1)*, 417-420, 1992.

Holzworth, R.H., and C.-I. Meng, Mathematical representation of the auroral oval, *Geophys. Res. Lett.*, *2*, 377-80, 1975.

Hughes, W. J., The effect of the atmosphere and ionosphere on long period magnetospheric micropulsations, *Planet. Space Sci.*, *22*, 1157, 1974.

Itonaga, M., A. Yoshikawa, and K. Yumoto, One-dimensional transient response of the inner magnetosphere at the magnetic equator, 2, Analysis of waveforms, *J. Geomagn. Geoelectr.*, *49*, 49-68, 1997.

Lee, D.-H., On the generation mechanism of Pi2 pulsations in the magnetosphere, *Geophys. Res. Lett.*, *24*, 583, 1998.

Lysak, R. L., and C. T. Dum, Dynamics of magnetosphere-ionosphere coupling including turbulent transport, *J. Geophys. Res.*, *88*, 365, 1983.

Meir-Jedrzejowicz, W. A. C., and W. J. Hughes, Phase skipping and packet structure in geomagnetic pulsation signals, J. Geophys. Res., *85*, 6888, 1980.

Olson, J. V., and G. Rostoker, Pi2 pulsations and the auroral electrojet, *Planet. Space Sci.*, *23*, 1129-1139, 1978.

Osaki, H., K. Takahashi, H. Fukunishi, T. Nagatsuma, H. Oya, A. Matsuoka, and D. K. Milling, Pi2 pulsations observed from the Akebono satellite in the plasmasphere, *J. Geophys. Res.*, *103*, 17605-17615, 1998.

Pashin, A. B., K. H. Glassmeier, W. Baumjohann, O. M. Raspopov, A. G. Yahnin, H. J. Opgenoorth, and R. J. Pellinen, Pi2 magnetic pulsations and the substorm current wedge, *J. Geophys. Res.*, *89*, 5489-5494, 1984.

Pekrides, H., A. D. M. Walker, and P. R. Sutcliffe, Global modeling of Pi2 pulsations, *J. Geophys. Res.*, *102*, 14343-14354, 1997

Rostoker, G., and J. V. Olson, Pi2 micropulsations as indicators of substorm onsets and intensifications, *J. Geomagn. Geoelectr.*, *30*, 135-147, 1978.

Saito, T., Geomagnetic pulsations, *Space Sci. Rev.*, *10*, 319-412, 1969.

Saito, T., T. Sakurai, and Y. Koyama, Mechanism of association between Pi2 pulsation and magnetospheric substorm, *J. Atmos. Terr. Phys.*, *38*, 1265, 1976.

Saka, O., K. Okada, O. Watanabe, D. N. Baker, G. D. Reeves, and R. D. Belian, Pi2-associated particle flux and magnetic field modulations in geosynchronous altitudes, *J. Geophys. Res.*, *102*, 11363-73, 1996.

Sakurai, T., and R. L. McPherron, Satellite observations of Pi2 activity at synchronous orbit, *J. Geophys. Res.*, *88*, 7015-7027, 1983.
Sakurai, T., and T. Saito, Magnetic pulsation Pi2 and substorm onset, *Planet. Space Sci.*, *24*, 573, 1976.
Sergeev, V. A., R. C. Elphic, F. S. Mozer, A. Saint-Marc, and J. A. Sauvaud, A two-satellite study of nightside flux transfer events in the plasma sheet, *Planet. Space Sci.*, *40*, 1551, 1992.
Sergeev, V. A., V. Angelopoulos, J. T. Gosling, C. A. Cattell, and C. T. Russell, Detection of localized, plasma depleted flux tubes or bubbles in the midtail plasma sheet, *J. Geophys. Res*, *101*, 10817-26, 1996.
Shiokawa, K., W. Baumjohann, and G. Haerendel, Braking of high-speed flows in the near-Earth tail, *Geophys. Res. Lett.*, *24*, 1179-1182, 1997.
Shiokawa, K., W. Baumjohann, G. Haerendel, G. Paschmann, J. F. Fennell, E. Friis-Christensen, H. Luhr, G. D. Reeves, C. T. Russell, P. R. Sutcliffe, and K. Takahashi, High-speed ion flow, substorm current wedge, and multiple Pi2 pulsations. *J. Geophys. Res.*, *103*, 4491, 1998.
Singer, H. J., W. J. Hughes, P. F. Fougere, and D. J. Knecht, The localization of Pi2 pulsations: Ground-satellite observations, *J. Geophys. Res.*, *88*, 7029-7036, 1983.
Southwood, D. J., and W. J. Hughes, Concerning the structure of Pi2 pulsations, *J. Geophys. Res.*, *90*, 386-392, 1985.
Sutcliffe, P. R., and K. Yumoto, Dayside Pi 2 pulsations at low latitudes, *Geophys. Res. Lett.*, *16*, 887-890, 1989.
Sutcliffe, P. R., and K. Yumoto, On the cavity mode nature of low-latitude Pi2 pulsations, *J. Geophys. Res.*, *96*, 1543-1551, 1991.
Takahashi, K., S.-I. Ohtani, and K. Yumoto, Ampte CCE observations of Pi2 pulsations in the inner magnetosphere, *Geophys. Res. Lett.*, *19*, 1447-1450, 1992.
Takahashi, K., S.-I. Ohtani, and B. J. Anderson, Statistical analysis of Pi2 pulsations observed by the AMPTE CCE spacecraft in the inner magnetosphere, *J. Geophys. Res.*, *100*, 21,929-21,941, 1995.
Tsyganenko, N.A., A magnetospheric magnetic field model with a warped tail current sheet, *Planet. Space Sci.*, *37*, 5-20, 1989.
Yoeman, T. K., M. P. Freeman, G. D. Reeves, M. Lester, and D. Orr, A comparison of midlatitude Pi2 pulsations and geostationary orbit particle injections as substorm indicators, *J. Geophys. Res.*, *99*, 4085-4093, 1994.
Yumoto, K., K. Takahashi, T. Saito, F. W. Menk, B. J. Fraser, T. A. Potemra, and L. J. Zanetti, Some aspects of the relation between Pi 1-2 magnetic pulsations observed at L = 1.3-2.1 on the ground and substorm-associated magnetic field variations in the near-Earth magnetotail observed by AMPTE CCE, *J. Geophys. Res.*, *94*, 3611-3618, 1989.
Zhu, X.M., and M. G. Kivelson, Global mode ULF pulsations in a magnetosphere with a nonmonotonic Alfvén velocity profile, *J. Geophys. Res.*, *94*, 1479-1485, 1989.

L. Kepko and M. Kivelson, Department of Earth and Space Sciences, University of California, Los Angeles, CA 90095-1567. (lkepko@igpp.ucla.edu)

(Received May 21, 1999; revised July 23, 1999; accepted August 11, 1999.)